Appl. Phys. A
DOI 10.1007/s00339-014-8346-y

**Applied Physics A**
**Materials Science & Processing**

# Investigation of the spontaneous emission rate of perylene dye molecules encapsulated into three-dimensional nanofibers via FLIM method

**Sabriye Acikgoz · Mustafa M. Demir · Ece Yapasan · Alper Kiraz · Ahmet A. Unal · M. Naci Inci**

Received: 26 December 2013 / Accepted: 23 February 2014
© Springer-Verlag Berlin Heidelberg 2014

**Abstract** The decay dynamics of perylene dye molecules encapsulated in polymer nanofibers produced by electrospinning of polymethyl methacrylate are investigated using a confocal fluorescence lifetime imaging microscopy technique. Time-resolved experiments show that the fluorescence lifetime of perylene dye molecules is enhanced when the dye molecules are encapsulated in a three-dimensional photonic environment. It is hard to produce a sustainable host with exactly the same dimensions all the time during fabrication to accommodate dye molecules for enhancement of spontaneous emission rate. The electrospinning method allows us to have a control over fiber diameter. It is observed that the wavelength of monomer excitation of perylene dye molecules is too short to cause enhancement within nanofiber photonic environment of 330 nm diameters. However, when these nanofibers are doped with more concentrated perylene, in addition to monomer excitation, an excimer excitation is generated. This causes observation of the Purcell effect in the three-dimensional nanocylindrical photonic fiber geometry.

S. Acikgoz · M. N. Inci
Department of Physics, Bogazici University, 34342 Istanbul, Turkey

S. Acikgoz (✉)
Department of Material Science and Engineering, Karamanoğlu Mehmetbey University, 70100 Karaman, Turkey
e-mail: sabriyeacikgoz@kmu.edu.tr

M. M. Demir
Department of Materials Science and Engineering, Izmir Institute of Technology, 35430 Izmir, Turkey

E. Yapasan
Department of Chemistry, Izmir Institute of Technology, 35430 Izmir, Turkey

A. Kiraz
Department of Physics, Koc University, 34450 Istanbul, Turkey

A. A. Unal
Helmholtz-Zentrum Berlin für Materialien und Energie, 12489 Berlin, Germany

## 1 Introduction

According to the Fermi's Golden rule, properties of the spontaneous emission depend not only on the quantum mechanical parameters of the emitter, but also on the density of propagating photon modes in the emitter's photonic environment. The problem of spontaneous emission decay rate of a molecule in the presence of various dielectric nanobodies like spheroidal and cylindrical has been studied considerably over the past few decades. Carminati et al. [1] has successfully derived an analytical procedure to explain the distance dependence of the spontaneous emission decay rate for spheroidal dielectric nanobodies, which demonstrates that the nonradiative decay rate follows an $R^{-6}$ dependence at short range; where $R$ is the distance between the emitter and the center of the nanoparticle. Dielectric optical nanofibers and carbon nanotubes are important examples of the cylindrical nanocavities. The influence of such a cylindrical geometry is investigated either for an atom being confined inside or planted outside the cavity [2, 3]. Moreover, the spontaneous emission rate of a dipole emitter can be altered by suitably modifying its photonic environment. Purcell [4] proposed that the mode structure of the vacuum field could be dramatically altered in a cavity. When a dipole is in resonance with a high-quality low-volume cavity mode, its spontaneous emission rate is enhanced. This is known as the Purcell effect. Modifications on the radiative decay

Published online: 12 March 2014

rates were also observed when emitters were between two flat substrates or between mirrors of high-finesse optical cavities and in whispering gallery mode resonators [5–7].

Photonic structures with wavelength-scale dimensions offer interesting opportunities to engineer the optical properties of embedded emitters. Particularly, for dimensions smaller than the wavelength of light, the strong modification of the local photonic density of states alters the photophysical properties of emitters such as decay rate, quantum yield and photobleaching rate [8]. For example, the spontaneous emission rate enhancement of molecules which are placed inside the nanometer-scale gap of plasmonic waveguide is experimentally demonstrated [9]. Moreover, in the case of the organic dye impregnated nanofibers, the nanoconfined organic dyes undergo a charge or energy transfer, resulting in the enhancement of the fluorescence signal [10, 11]. In addition, fluorescent nanofibers have potential use in chemical and bio-sensing applications [12, 13]. The sensing performance is improved by the extended effective surface area of the nanofibers.

Perylene is a brown crystalline polycyclic aromatic hydrocarbon with the chemical formula $C_{20}H_{12}$. It can be soluble in most of the organic solvents and its blue fluorescence in solution seen even in visible light. High fluorescence quantum yield, photostability and efficient carrier mobility also make perylene an excellent candidate for use in organic electroluminescent diodes [14]. Perylene molecules form a characteristic excimer in excited state; therefore, they are widely used as fluorescent probe in different research fields [15]. Due to red color emission of excimer, perylene molecules have been used in several biological investigations as well as DNA detection and probing of physical status of membrane [16, 17]. Excimer formation processes of perylene molecules have been studied for a long time under various conditions such as in solution, in crystalline, in thin polymer film, in polymer matrix, in LB film [18–24].

In this work, we studied excimer formation of perylene molecules within three-dimensional cylindrical nanofibers (NFs). They are produced using electrospinning, which is a straightforward and cost-effective method to produce novel fibers with diameters in the range of nano to micrometer [25]. Moreover; it is a convenient method, which allows for manufacturing of regular and long nanofibers of the order of 10 cm. The electrospinning process and the resulting fiber morphology depend on the solution properties (e.g., viscosity, conductivity, surface tension, permittivity, and boiling point) and operating conditions (e.g., applied voltage, spinneret-to-collector distance, and flow rate) [26]. These properties of electrospun nanofibers make them suitable for a wide range of applications such as medicine, tissue engineering, drug delivery control, filtration, sensors, energy and environmental protection [27–32]. The modification of the spontaneous emission rate of perylene dye molecules embedded in Polymethyl methacrylate (PMMA)-based NFs is experimentally demonstrated and excimer formation map of perylene molecules within NFs is obtained via confocal fluorescence lifetime imaging microscopy (FLIM) method.

## 2 Experimental section

### 2.1 Polymerization of MMA and electrospinning of PMMA/perylene nanofibers

Methyl methacrylate (MMA) stabilized with 10–20 ppm hydroquinone monomethyl ether is obtained from Fluka. It is freshly distilled under vacuum prior to polymerization. Benzoyl peroxide (BPO) is also provided from Fluka and used as initiator. BPO is recrystallized from methanol. Perylene dye is bought from Fluka. Dimethyl formamide (DMF) and tetrahydrofurane (THF) are obtained from Riedel Haen and used as they are without further purification.

MMA is distilled under vacuum. The round bottom flask containing equimolar MMA–DMF mixture is placed into a preheated bath at 60 °C. BPO is used as radical source. The weight average molecular weight of PMMA was found to be 673 ± 144 and 420 ± 48 kDa, respectively. The mixture is subjected to freeze–thaw process three times and polymerization is carried out under vacuum for 5 h. It is then quenched to room temperature and polymerization is stopped when the reactor is opened. For purification, PMMA is dissolved in THF and the solution is precipitated in methanol. The precipitated polymer is dried under vacuum at room temperature.

PMMA is dissolved in DMF at a concentration of 2 % (w/w). Perylene dye is codissolved in the same solution with different concentrations ranging from 0.1, 0.2, 0.3, 0.4 and 0.5 % (w/w). The polymer/perylene solutions were subjected to electrospinning using a classical horizontal electrospinning setup [33]. As a counter electrode where fibers are collected, continuous Al foil or a parallel positioned two metal strips with an air gap are used. Depending on geometry of the electrode, different arrangements of fibers are obtained. Instrumental parameters in electrospinning are as follows: flow rate, 3 mL/h; applied potential difference, 12 kV; and spinning distance, 10–15 cm. Weight average molecular weight of PMMA is obtained by dynamic light scattering (DLS, Nano ZS Malvern Worcestershire). The morphology of the fiber mats (diameter and shape of fibers, arrangement of fibers) is studied using scanning electron microscopy (SEM, FEI Quanta 250, Oregon). Average fiber diameter (AFD) is obtained from statistical treatment of SEM images by measuring the diameter of typically not less than 50 fibers with the help of ImageJ [34].

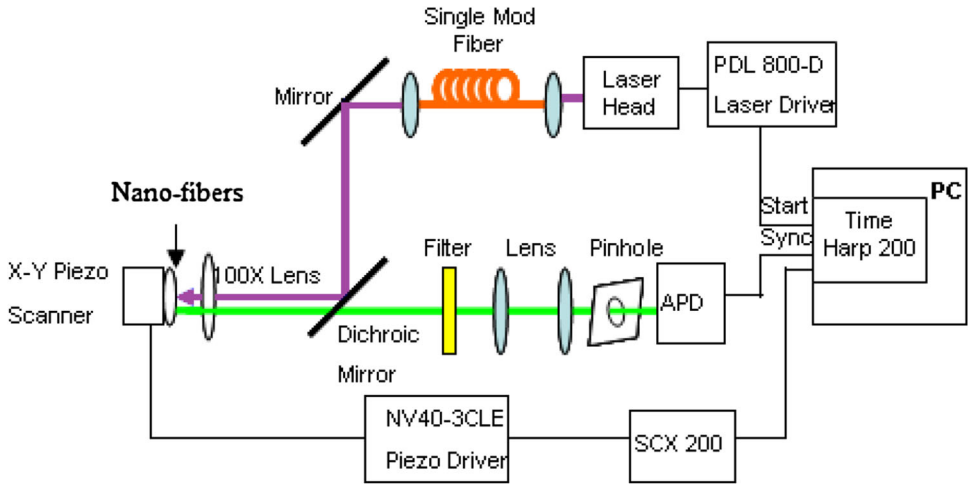


**Fig. 1** Optical FLIM setup

### 2.2 Time-resolved lifetime and fluorescence intensity measurements

Time-resolved fluorescence lifetime and fluorescence intensity measurements are performed using a TimeHarp 200 PC-Board system (Picoquant, GmbH) and a fiber optic spectrometer (USB4000-VIS–NIR Ocean Optics), respectively (see Fig. 1). The excitation source used in the experiment is an ultraviolet pulsed diode laser head with a wavelength of 405 nm (LDH-C-D-405 Picoquant, GmbH). To obtain a Gaussian beam illumination, a single mode optical fiber is used as a waveguide (Thorlabs, S405-HP). The excitation light is focused onto the sample using a microscope objective of 0.55 numerical apertures with a working distance of 10.1 mm (Nikon, ELWD 100X). A pinhole, which has a diameter 75 μm, is placed to focal plane, to increase the resolution of the FLIM images. In the confocal FLIM setup, a xy piezo scanner from Piezosystem Jena, which allows a scan range of 100 × 100 $\mu m^2$ (NV40-3CLE), and SCX 200 (Picoquant, GmbH) fluorescence lifetime imaging controller are used for NFs surface scanning. Fluorescence lifetimes are calculated pixel-by-pixel using SymPho Time software (Picoquant, GmbH).

For multi-exponential fluorescence decay fitting, FluoFit computer program (Picoquant, GmbH) is used. The fluorescence intensity decays are recovered from the frequency-domain data in terms of a multi-exponential model,

$$I(t) = \sum_{i=1}^{n} A_i \exp(-t/\tau_i) \tag{1}$$

where $A_i$ is the amplitude of each component and $\tau_i$ is its lifetime. The fractional contribution of each component to the steady-state intensity is described by

$$f_i = \frac{A_i \tau_i}{\sum_j A_j \tau_j} \tag{2}$$

The intensity weighted average lifetime is represented as

$$\langle \tau \rangle = \sum_i f_i \tau_i \tag{3}$$

and the amplitude weighted lifetime is given by

$$\bar{\tau} = \frac{\sum_i A_i \tau_i}{\sum_i A_i}. \tag{4}$$

## 3 Results and discussion

PMMA/perylene solutions at different concentrations were subjected to electrospinning at 1 kV/cm. Figure 2 presents overview SEM images of nonwoven perylene-doped PMMA fibers. Average fiber diameter ranges from 0.3 to 0.4 μm. It was found to be independent of perylene concentration in PMMA at least in the concentration range we employed in this study. The fibers were also imaged by fluorescence microscope (FM, panel a of Fig. 3) and confocal fluorescence lifetime imaging microscope (FLIM, panel b of Fig. 3).

Nanofibers shown in Fig. 2 are functionalized by aromatic perylene dye molecules. The fluorescence intensity and spontaneous emission rate of perylene are studied in the optical setup shown in Fig. 1. The concentration of the perylene molecules in the nanofibers is controlled by adding various concentrations of fluorescent molecules to the polymer solution. Perylene molecules are uniformly distributed within and along the nanofibers. Fluorescence spectra of perylene in PMMA-based nanofiber at five different concentrations are shown in Fig. 4. The five samples have the same optical density. The fluorescence emission spectrum of a dilute perylene solution is characterized by an ensemble of three major vibronic bands with well defined peaks at 450, 480 and 510 nm, respectively. This spectrum is essentially a structured mirror image of the absorption

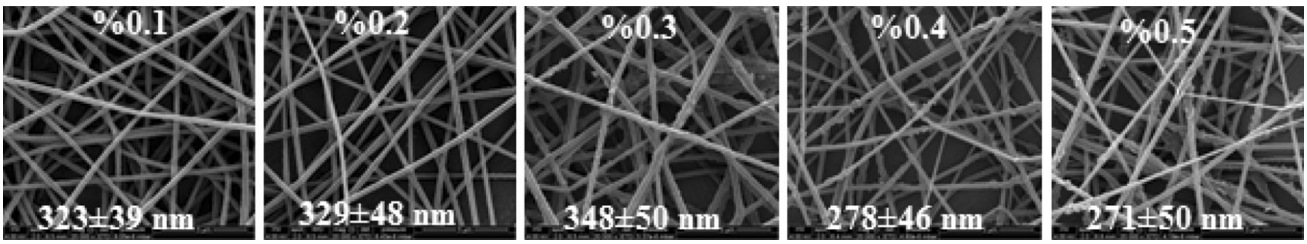


**Fig. 2** SEM images of fibers electrospun from PMMA/perylene dye solutions. Dye content in PMMA is given wt% as the inset of each image

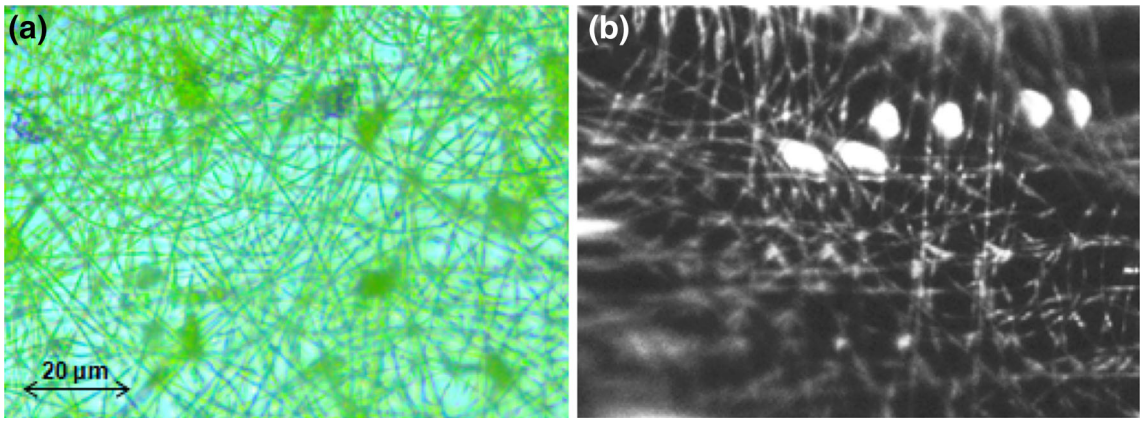


**Fig. 3** Representative FM (**a**) and FLIM (**b**) images (12.2 × 9.0 μm) of perylene-doped NFs

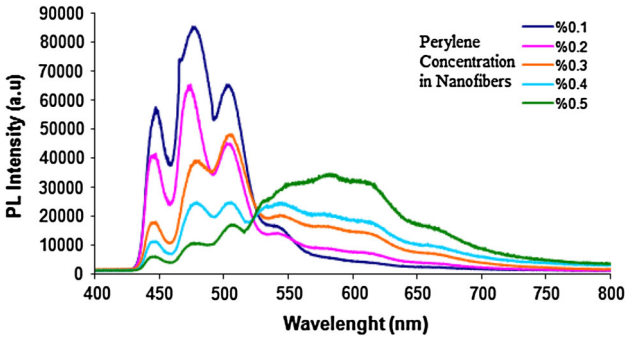


**Fig. 4** Fluorescence spectra of perylene in PMMA-based nanofiber at different concentrations

spectrum, as would be expected for relaxation from the excited singlet states of isolated molecules. Fluorescence spectrum of aromatic hydrocarbon dye molecules, like perylene, depends on the concentration of dye molecules. In many cases, concentration quenching of the molecular fluorescence is accompanied by the appearance of a new emission band which is red-shifted compared to the fluorescence of the uncomplexed molecules. Excimer is an excited state dimer and results from the interaction between an excited singlet state and an unexcited molecule. Excimer emission spectrum is broad and structureless with the peak around 580 nm. Under increasing concentrations of perylene, the fluorescence spectra are red-shifted. Unstructured emission is observed at concentrations of 0.3, 0.4 and 0.5 mol % perylene-doped nanofibers.

To measure the decay parameters of free perylene dye molecules, they are doped on a microscope slide at two different concentrations: highly concentrated and dilute. The time-resolved fluorescence lifetime of the perylene dye molecule is performed using the PCI-Board system (TimeHarp 200, PicoQuant). The measurement of the fluorescence lifetime is based on the time correlated single photon counting (TCSPC) method. In this method, the time between the detected single photon of the fluorescence (start signal) and the excitation laser pulse (stop signal) is measured. The measured data are plotted as a fluorescence lifetime histogram. Decay parameters are determined using the double exponential tailfit model, and the best fits are obtained by minimizing $\chi^2$ values. At high concentration, perylene exhibits excimer formation and the intensity weighted fluorescence lifetime of perylene monomer band is measured as 4.1326 ns, while that of excimer band emission is 12.2095 ns as seen in Fig. 5 and 6, respectively. The excited state lifetime of the excimer species is significantly longer than that of the monomer; therefore, fluorescence lifetime measurements are typically used to confirm the presence of excimers.

The versatility of the fluorescence lifetime method allows its application to diverse areas of study, including but not limited to materials science, arts, aeronautics,

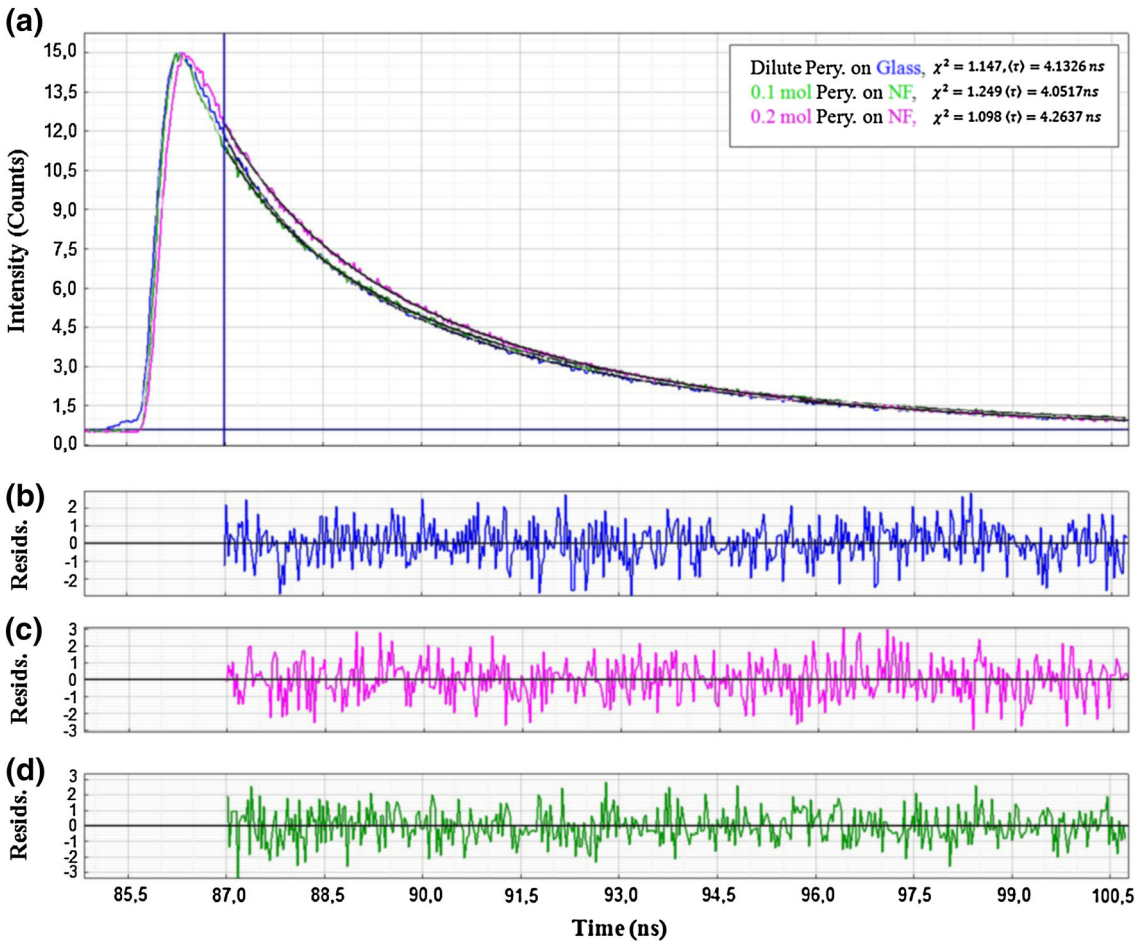


**Fig. 5** **a** Fitting and calculation of decay parameters of Perylene on (*blue*) glass, (*pink*) 0.2 mol Perylene on NF, (*green*) 0.1 mol Perylene on NF. (*Continuous line*) indicate multi-exponential fitting *curve*. Residuals for fittings on (**b**) glass, (**c**) 0.2 mol Perylene on NF, (**d**) 0.1 mol Perylene on NF

agriculture, forensics, biology and medicine. It is known that the presence of dielectric interfaces influences the radiative transition frequencies and decay rates. According to the studies on the spectroscopic characteristics of an atom surrounding with a cavity, fluorescence lifetime of atom depends on the dimensions of the cavity. If the dimensions of the cavity are larger than or comparable to the radiation wavelength, the spontaneous emission rate of the atom changes considerably due to resonant modes (whispering gallery modes) [35]. However, in the case of nanocavities, whose dimensions are much smaller than the radiation wavelength, surface curvature and quadruple transitions as well as the plasmon resonances become effective on the spontaneous decaying rates. It is predicted by Purcell that an atom in a smaller wavelength-size cavity can radiate much faster than in the free space [36].

In this work, the fluorescence lifetime of perylene dye molecules in a smaller wavelength-size cavity is investigated. To observe the wavelength-dependent photonic interactions between dye molecules and nanofibers, nanofiber diameter is specially fabricated fixed around 330 nm. For fiber diameters below ~300 nm, the size is hard to determine due to diffraction and the resolution of our confocal microscope is not enough to obtain FLIM images of these types of nanofibers. Therefore, we have performed all the time-resolved fluorescent lifetime experiments for such nanofibers. While the monomer emission is observed at a wavelength about 400 nm for 0.1 and 0.2 mol perylene-doped nanofibers, the excimer emission appears at a wavelength about 600 nm for concentrated (0.3, 0.4 and 0.5 mol) perylene-doped nanofibers. Time resolved experiments show that, the average fluorescence lifetime of perylene monomer emission remains almost the same for the fiber diameter about 330 nm. The fluorescence lifetime decay curves of dilute perylene molecules on PMMA-based NF and microscope slide are given in Fig. 5. The perylene monomer fluorescence decay curves are also analyzed using FluoFit software and calculated decay parameters are given in Table 1. It is observed that the average lifetime values are centered

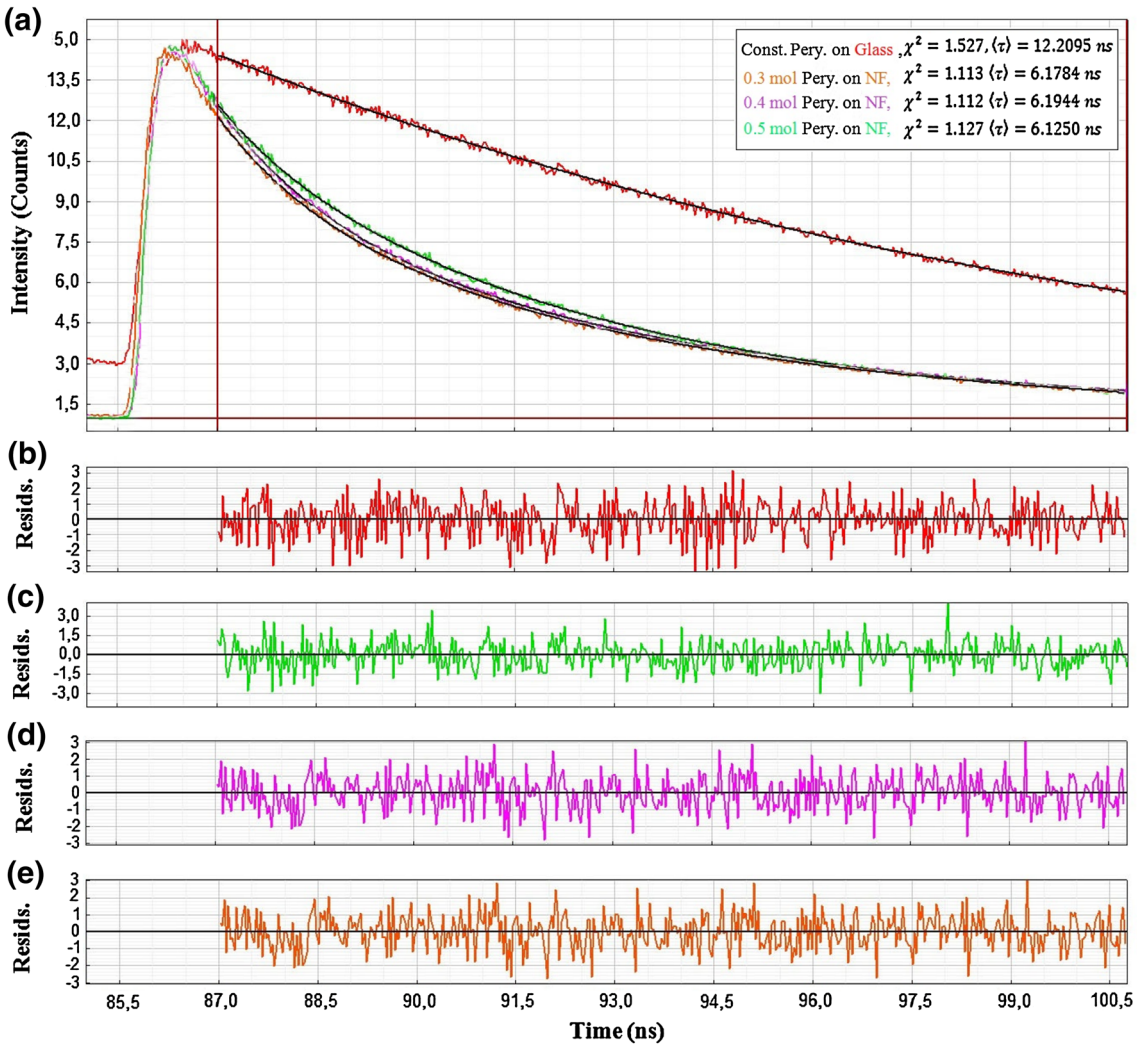


**Fig. 6** **a** Fitting and calculation of decay parameters of Perylene on (*red*) glass, (*green*) 0.5 mol Perylene on NF, (*pink*) 0.4 mol Perylene on NF, (*orange*) 0.3 mol Perylene on NF. (*Continuous line*) indicate multi-exponential fitting *curve*. Residuals for fittings on (**b**) glass, (**c**) 0.5 mol Perylene on NF, (**d**) 0.4 mol Perylene on NF, (**e**) 0.3 mol Perylene on NF

**Table 1** Monomer emission decay parameters of perylene

| Sample | $A_1$ (au) | $\tau_1$ (ns) | $A_2$ (au) | $\tau_2$ (ns) | $\langle\tau\rangle^a$(ns) | $\bar{\tau}^b$(ns) | $\chi^2$ |
|---|---|---|---|---|---|---|---|
| Glass | 7,746.3 | 4.4833 | 3,491.8 | 1.1820 | 4.1326 | 3.4576 | 1.147 |
| NF +0.1 Perylene | 8,956.0 | 4.3019 | 2,820.0 | 1.1979 | 4.0517 | 3.5586 | 1.249 |
| NF +0.2 Perylene | 7,856.6 | 4.5349 | 2,717.6 | 1.1375 | 4.2637 | 3.6618 | 1.098 |

[a] The intensity weighted average lifetime (Eq. 3)

[b] The amplitude weighted average lifetime (Eq. 3)

about 4.0–4.3 ns. Because of the fact that the dimension of a nanofiber is comparable to the monomer emission wavelength, the presence of nanofibers does not become effective on the decay rates of a single perylene molecule.

On the other hand, the time-resolved experiments reveal a significant modification of the decay rate of excimer emission of perylene molecules for diameters (∼300 nm) below the wavelength of radiation (∼600 nm). The fluorescence lifetime of perylene molecules decreases from 12.2095 to 6.1250 ns. In Fig. 6, the fluorescence lifetime decay curves are given and calculated decay parameters are summarized in Table 2. The great decrease in the fluorescence lifetime of the concentrated perylene-doped NF is likely due to much longer wavelength of excimer emission.

Particularly, for dimensions below the wavelength of light, the associated strong modification of the local photonic density of states alters the photophysical properties of the emitters.

Fluorescence lifetime imaging microscopy (FLIM) is an imaging technique for producing an image based on the differences in the exponential decay rate of the fluorescence from a fluorescent sample. FLIM is quite an innovation because it allows fluorescence lifetime sensitivities to be monitored in a spatially distinct manner in living cells as well as for other chemical processes. Moreover, FLIM can probe the local environments of fluorophores such as the local pH, refractive index, ion and oxygen concentration without the need for ratio metric measurements. FLIM can be performed with two distinct methods. In the first method, the fluorescence intensity for each pixel is determined after a short time interval via time-gated experiments and an intensity map is produced. This method offers the potential to eliminate background fluorescence and enhance imaging contrast. The other method is performed by measuring the fluorescence lifetime for each pixel and generating a lifetime map of the object. Three-dimensional information can be obtained by FLIM technique

**Table 2** Excimer emission decay parameters of perylene

| Sample | $A_1$ (au) | $\tau_1$ (ns) | $A_2$ (au) | $\tau_2$ (ns) | $\langle\tau\rangle^a$(ns) | $\bar{\tau}^b$(ns) | $\chi^2$ |
|---|---|---|---|---|---|---|---|
| Glass | 16,100.3 | 11.6834 | −2,657.8 | 6.285 | 12.2095 | 12.7507 | 1.527 |
| NF +0.3 Perylene | 8,138.2 | 6.6873 | 3,752.7 | 1.6184 | 6.1784 | 5.0876 | 1.113 |
| NF +0.4 Perylene | 8,120.9 | 6.7090 | 3,773.7 | 1.6265 | 6.1944 | 5.0966 | 1.112 |
| NF +0.5 Perylene | 8,276.7 | 6.4349 | 1,927.5 | 2.1585 | 6.1250 | 5.6271 | 1.127 |

[a] The intensity weighted average lifetime (Eq. 3)

[b] The amplitude weighted average lifetime (Eq. 4)

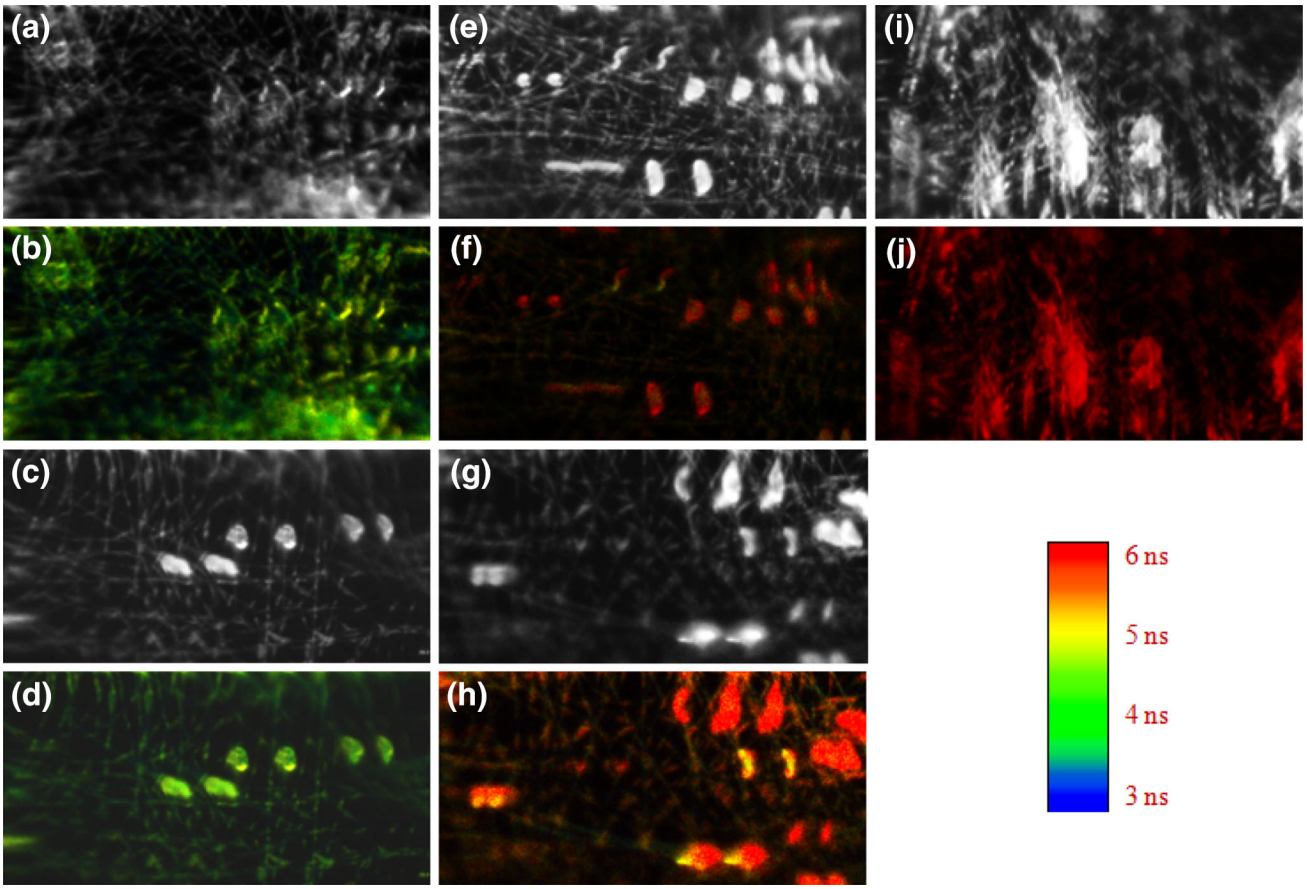


**Fig. 7** **a**, **b** 0.1 mol Perylene doped NF confocal intensity and FLIM image (**c**, **d**) 0.2 mol Perylene doped NF confocal intensity and FLIM image (**e**, **f**) 0.3 mol Perylene doped NF confocal intensity and FLIM image (**g**, **h**) 0.4 mol Perylene doped NF confocal intensity and FLIM image (**i**, **j**) 0.5 mol Perylene doped NF confocal intensity and FLIM image

and FLIM lifetime maps are generally used to monitor the functional changes due to environmental factors.

FLIM method is used to obtain individual lifetime values of aromatic perylene dye molecules encapsulated into PMMA-based nanofibers and to construct an excimer formation map of these dye molecules. The confocal fluorescence intensity and FLIM images of perylene dye molecules encapsulated into three-dimensional polymer-based NFs are given in Fig. 7. FLIM images are displayed using a continuous pseudocolor scale ranging from 3 to 6 ns (from blue to red). In other words, color of the images represents fluorescence lifetime of perylene dye molecules within NFs. Moreover, the size of every FLIM figure is 500 × 250 pixel (12.2 × 6.1 μm). Our picosecond time-resolved experiments show that the fluorescence lifetime of perylene monomer and excimer emission within a confined environment (NFs) are about 4 and 6 ns, respectively. In FLIM images, the green color represents monomer emission lifetimes of about 4 ns and the red color excimer emission lifetimes of about 6 ns. For dilute perylene concentration, green color is dominant as seen in Fig. 7b and d. When the concentration of perylene dye molecules within NFs is increased, excimer formation starts and the color distribution in the FLIM image shifts from green to red. The resolution of our homemade and open frame FLIM microscope is about 200 nm. Therefore, a single nanofiber is clearly observed in dilute perylene dye-doped FLIM images. When the dye concentration is increased, the adhesion of nanofibers occurs and the resolving power of our FLIM images reduces. In Fig. 7j, it is observed that the fluorescence lifetime of perylene excimer emission in a single nanofiber and that in the adhesive nanofibers has the same value. Consequently, the adhesion of nanofiber is not effective on the fluorescence lifetime values.

The existence of perylene excimer in NFs is confirmed for the first time by observing the difference between the decay times of excimer and monomer fluorescence with fluorescence lifetime imaging method. The use of FLIM is more robust and reliable than fluorescence intensity-based methods, since FLIM is unaffected by variations of illumination intensity and photobleaching.

## 4 Conclusion

In this work, we report the association of perylene as model hydrophobic molecules by PMMA-based nanofibers that assembled into cylindrical nanostructures using electrospinning. Monomer emission of perylene is unaffected by NF which has a diameter of about 330 nm and its lifetime remains unchanged. When the concentration of perylene increases, molecular motion of the perylene molecule is restricted within nanofibers so that excimer emission arises from the partially overlapped conformation. As compared to free excimer emission of perylene, time-resolved experiments show that the fluorescence lifetime of excimer emission of perylene, which is encapsulated into NFs, gets shortened dramatically. Such a decrease in the lifetime is measured to be almost 50 %, which indicates that the excimer emission of perylene molecules is more sensitive to change in the surrounding environment due to its longer wavelength. This work ensures that the fluorescence characteristics of an excimer can be modified due to the Purcell effect and electrospun NFs are such suitable materials for investigating the effects of different local photonic environments. Conversely, FLIM technique is used to record high-resolution optical images of the electrospun NFs and to obtain excimer formation map of perylene molecules within NFs.

**Acknowledgments** This work was supported by TUBITAK under contract number 106T011, Bogazici University and Karamanoğlu Mehmetbey Universities Research Funds under contract numbers 13B03P4 and 01-M-13, respectively.

## References

1. R. Carminati, J.J. Greffet, C. Henkel, J.M. Vigoureux, Opt. Commun. **261**, 368 (2006)
2. C. Dekker, Phys. Today **52**, 22 (1999)
3. V.V. Klimov, M. Ducloy, Phys. Rev. A **69**, 13812 (2004)
4. E.M. Purcell, Phys. Rev. **69**, 681 (1946)
5. R.G. Hulet, E.S. Hilfer, D. Kleppner, Phys. Rev. Lett. **55**(20), 2137 (1985)
6. F. De Martini, G. Innocenti, G.R. Jacobovitz, P. Mataloni, Phys. Rev. Lett. **59**, 2955 (1987)
7. H.B. Lin, J.D. Eversole, C.D. Meritt, A.J. Campillo, Phys. Rev. A **45**, 6756 (1992)
8. N. Tomczak, S. Gu, M. Han, N.F. Hulst, G.J. Vancso, Eur. Polym. J. **42**, 2205 (2006)
9. V.J. Sorger, N. Pholchai, E. Cubukcu, R.F. Oulton, P. Kolchin, C. Borschel, M. Gnauck, C. Ronning, X. Zhang, Nano Lett. **11**, 4907 (2011)
10. H. Yu, H. Wang, T. Li, R. Che, Appl. Phys. A **108**, 223 (2012)
11. K.J. Lee, J.H. Oh, Y. Kim, J. Jang, Adv. Mater. **18**, 2216 (2006)
12. X. Liu, X. Zhang, R. Lu, P. Xue, D. Xu, H. Zhou, J. Mater. Chem. **21**, 8756 (2011)
13. B. Law, R. Weissleder, C.H. Tung, Bioconjug. Chem. **18**, 1701 (2007)
14. B. Ding, W. Zhu, X. Jiaing, Z. Zhang, Solid State Commun. **148**(5), 226 (2008)
15. K.A. Nelson, D.D. Dlott, M.D. Fayer, Chem. Phys. Lett. **64**(1), 88 (1979)
16. W. Tuntiwechapikul, M. Salazar, Biochemistry **40**, 13652 (2001)
17. W. Tuntiwechapikul, T. Taka, M. Béthencourt, L. Makonkawkeyoon, L.T. Randall, Bioorg. Med. Chem. Lett. **16**, 4120 (2006)
18. R. Katoh, S. Sinha, S. Murata, M. Tachiya, J. Photochem. Photobiol. A **145**, 23 (2001)
19. H. Auweter, D. Ramer, B. Kunze, H.C. Wolf, Chem. Phys. Lett. **85**(3), 325 (1982)
20. H. Nishimura, A. Matsui, M. Iemura, J. Phys. Soc. Jpn. **51**, 1341 (1982)
21. H. Tachikawa, L.R. Faulkner, Chem. Phys. Lett. **39**, 436 (1976)

22. Z. Salamon, H. Bassler, Chem. Phys. **100**, 393 (1985)
23. D. Weiss, R. Kietzmann, J. Mahrt, B. Tufts, W. Storck, F. Willing, J. Phys. Chem. **96**, 5320 (1992)
24. S. Akimoto, A. Ohmori, I. Yamazaki, J. Phys. Chem. B **101**, 3753 (1997)
25. D.H. Reneker, A.L. Yarin, E. Zussman, H. Xu, Adv. Appl. Mech. **41**, 43 (2006)
26. H. Matsumoto, A. Tanioka, Membranes **1**(3), 249 (2011)
27. W. Liu, S. Thomopoulos, Y. Xia, Adv. Healthc. Mater. **1**, 10 (2012)
28. R. Vasita, D.S. Katti, Int. J. Nanomed. **1**(1), 15 (2006)
29. D.G. Yu, L.M. Zhu, K. White, C.B. White, Health **1**(2), 67 (2009)
30. X.H. Qin, S.Y. Wang, J. Appl. Polym. Sci. **102**, 1285 (2006)
31. B. Ding, M. Wang, J. Yu, G. Sun, Sensors **9**, 1609 (2009)
32. V. Thavasi, G. Singh, S. Ramakrishna, Energy Environ. Sci. **1**, 205 (2008)
33. M.M. Demir, I. Yilgor, E. Yilgor, B. Erman, Polymer **43**(11), 3303 (2002)
34. National Institutes of Health: Public domain software to be downloaded from http://rsb.info.nih.gov/ij
35. A.G. Vitukhnovsky, M.I. Such, J.G. Warren, M.C. Petty, Chem. Phys. Lett. **184**, 235 (1991)
36. V.B. Braginsky, M.L. Gorodetsky, V.S. Ilchenko, Phys. Lett. A **137**, 393 (1989)